https://doi.org/10.5194/egusphere-2025-6334
Preprint. Discussion started: 20 January 2026
© Author(s) 2026. CC BY 4.0 License.

# Contributions of supraglacial lakes to the Greenland Ice Sheet melting

Alessandro Cotronei[1], Ulrike Feudel[2], and Angelika Humbert[3]

[1] Department of Mathematics and Statistics, UiT - The Arctic University of Norway, Forskningsparken 1, Tromsø, Norway
[2] Institute for Chemistry and Biology for the Marine Environment, Carl von Ossietzky University Oldenburg, Carl-von-Ossietzky-Straße 9 - 11, Oldenburg,Germany
[3] Alfred-Wegener-Institut Helmholtz Zentrum für Polar- und Meeresforschung, Am Alten Hafen 26, Bremerhaven, Germany

**Correspondence:** Alessandro Cotronei (a.cotronei@uit.no)

**Abstract.** The Greenland Ice Sheet is considered a potential tipping element in the Earth system, as it may undergo rapid and irreversible ice loss. The complete loss of the ice sheet would lead to significant sea-level rise, posing an existential risk to humanity. Supraglacial lakes on the ice sheet enhance melting by reducing surface albedo and increasing melt rates during summer. We develop a simple conceptual model to investigate this process. The model consists of three coupled partial differential equations describing the temporal evolution of ice, water, and snow thickness within a simplified physical domain of Greenland, all driven by the annual temperature cycle. Model integrations show that, under realistic conditions, the presence of supraglacial lakes accelerates local ice melting and modifies the long-term ice-sheet topography. Regions with recurrent lake formation exhibit greater elevation differences. Under Shared Socioeconomic Pathway warming scenarios, only the lowest-emission scenarios prevent the onset of a self-sustaining melt–elevation feedback that could ultimately lead to complete ice-sheet loss. These results highlight the critical role of supraglacial lakes in amplifying ice-sheet melt and suggest that their influence should be more explicitly represented in comprehensive climate and ice-sheet models.

## 1 Introduction

The Greenland Ice Sheet (GrIS) is a massive ice mass that covers most of Greenland's surface and contains enough ice to raise the sea level by $7.42 \pm 0.05$ m (Morlighem et al., 2017), if it melts entirely. In recent years, an increasing melting rate has been observed (Trusel et al., 2018), and there is some indication that Greenland might be approaching a tipping point, an abrupt and irreversible transition in the form of ice loss that may already have happened in the past (Boers, 2018; Boers et al., 2022). Assuming that ice ablation occurs at a rate of 8 mm $^{\circ}C^{-1}$ $day^{-1}$ for each positive degree day, future scenarios of increased emissions assuming a yearly mean temperature of 1 °C could cause a regime that would cause the complete melting of Greenland (considering an ice thickness of 3.5 km) in circa 1200 y, which is in the same order of magnitude of model prediction for the scenario of Greenland melting (Charbit et al., 2008). The GrIS may also warm before the end of the century to temperatures that, in the past, were associated with substantial ice loss (Masson-Delmotte et al., 2012).

The decline of the Greenland Ice Sheet can follow a range of pathways, including potentially catastrophic scenarios driven by complex feedback interactions (Zeitz et al., 2022). This underscores the importance of understanding the specific feedback

https://doi.org/10.5194/egusphere-2025-6334
Preprint. Discussion started: 20 January 2026
© Author(s) 2026. CC BY 4.0 License.

mechanisms and possible future trajectories of ice loss. Moreover, substantial melting of the GrIS could disrupt the Atlantic Meridional Overturning Circulation (AMOC), with far-reaching impacts on the global climate system (Cessi, 1994; Masson-Delmotte et al., 2012). Therefore, it is critical to investigate the processes that influence GrIS melting. One such process involves supraglacial lakes, which form on the ice surface during the warmest months and are thought to significantly accelerate meltwater runoff and ice sheet evolution (Sneed and Hamilton, 2007). The variety of characteristics of supraglacial lakes can be seen as a result of a complex process that involves the interplay of multiple components, such as temperature, albedo, and mechanical processes. In this study we employ a conceptual model of the Greenland Ice Sheet to more clearly understand the role of supraglacial lakes with relation to increasing temperatures in the context of global warming and climate change, especially in view of earlier findings suggesting that western Greenland was losing ice faster than other regions (Huybrechts et al., 1991), whereas more recent studies indicate that accelerated melting now affects the entire ice sheet (Khan et al., 2025), and all Greenland more than global means (Smith et al., 2019). This analysis is meant to contribute to a further understanding of possibly essential processes influencing the future of the Greenland Ice Sheet.

Supraglacial lakes usually form on the Greenland Ice Sheet near its Western margin in Spring and Summer, when the air temperature in some areas of Greenland increases over the melting point of ice, causing water to flow in the naturally occurring depressions in the ice profile. Once formed, a lower albedo than the surroundings characterizes the supraglacial lakes, and hence, absorbs more solar radiation that increases the melting rate of the underlying ice (Echelmeyer et al., 1991; Sneed and Hamilton, 2007), see Fig. 1. Eventually supraglacial lakes typically drain through moulins and fractures in the ice sheet (Hoffman et al., 2018), letting the water flow down due to gravity (seepage) (Stevens et al., 2015; Christoffersen et al., 2018; Chudley et al., 2019; Humbert et al., 2025). The water that drains through the ice sheet might make the ice of GrIS more fluid and might lubricate the ice sheet base, increasing the horizontal velocity of the ice mass and potentially increasing calving and ice loss (Zwally et al., 2002; Parizek and Alley, 2004; Maier et al., 2023).

Melt ponds are commonly observed on Arctic sea ice, where they play a significant role in the ice-albedo feedback mechanism, influencing the absorption of solar radiation and accelerating the melting of the ice. Despite being smaller in size, their effect is comparable to supraglacial lakes. Recent climate models that incorporate melt ponds on Arctic sea ice have demonstrated their importance for accurately simulating ice dynamics and regional climate patterns (Holland et al., 2012; Diamond et al., 2024). These models show how the darker color of melt ponds (caused by the low albedo of liquid water and their typical thicknesss of a few meters, which allow them to absorb more sunlight compared to the surrounding ice) amplifies surface melting. The presence of melt ponds on sea ice has been found to have a substantial impact on the timing of ice melt, the thickness of sea ice, and the overall sea ice extent, influencing both local and global climate systems (Holland et al., 2012).

However, when it comes to simulating the Greenland Ice Sheet, supraglacial lakes have received much less attention in climate models. While the formation of supraglacial lakes on Greenland has been well-documented in the warmer months, their incorporation into climate models has been relatively limited. Given the importance of supraglacial lakes for surface melting and their potential to influence the mass balance of the Greenland Ice Sheet, it is crucial to better understand and model their formation and evolution in a fashion that could be adapted from a climate model, too. This is the motivation behind our work, which aims to address the lack of detailed consideration of Greenland supraglacial lakes in state-of-the-art climate models.

https://doi.org/10.5194/egusphere-2025-6334
Preprint. Discussion started: 20 January 2026
© Author(s) 2026. CC BY 4.0 License.

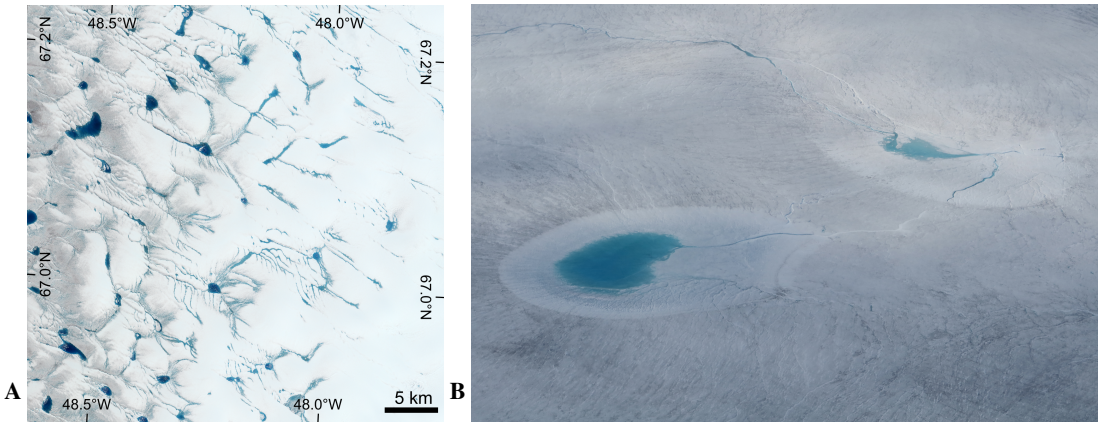


**Figure 1.** Optical images of supraglacial lakes on the Greenland Ice Sheet, showing (A) multiple lakes and (B) lakes that have drained with meltwater seeping through the ice. Picture credits: (A) Copernicus Sentinel-2, (B) U. Feudel (Uni Oldenburg, Germany).

Additional motivation for our work arises from the necessity to characterize better the melt elevation feedback (Levermann and Winkelmann, 2016) in Western Greenland, where supraglacial lakes may accelerate the melt rates of the GrIS. To bridge these gaps, we have developed a toy model to simulate the basic process of supraglacial lake formation on the Greenland Ice Sheet.

Our toy model represents a simplified but instructive version of how supraglacial lakes form and evolve on the Greenland Ice Sheet. By focusing on key factors such as surface temperature, ice characteristics, water flow and seasonal changes, the model aims to capture the fundamental physical processes that lead to the formation and drainage of supraglacial lakes. Although the model is not as complex or detailed as more advanced climate models, it provides a valuable tool for understanding the general dynamics. It can serve as a stepping stone toward integrating supraglacial lake processes into larger-scale simulations of the Greenland Ice Sheet.

## 2 The model

According to our aim to study the impact of supraglacial lakes on the Greenland Ice Sheet melting we model the interactions between the thickness of the ice sheet $I$, the thickness of the meltwater lake $W$, and the thickness of the snow $S$ under a temperature forcing $T$. We assume that these are the main variables that need to be taken into account, although additional impact factors like e.g. air pressure, air humidity and wind speed – all neglected here – might also influence the supraglacial lake formation (Lüthje et al., 2006b; Buzzard et al., 2018; Scagliarini et al., 2020). We formulate the primary interactions between $I$, $W$, $S$ and $T$ to develop a simplified yet meaningful model for supraglacial lake formation in Greenland. This approach allows us to describe the key dynamics governing meltwater accumulation and ice evolution while keeping the system computationally manageable. In the following, we outline the four evolution equations for the ice thickness $I$, the water thickness $W$, the snow thickness $S$ and the temperature $T$ in detail:

https://doi.org/10.5194/egusphere-2025-6334
Preprint. Discussion started: 20 January 2026
© Author(s) 2026. CC BY 4.0 License.

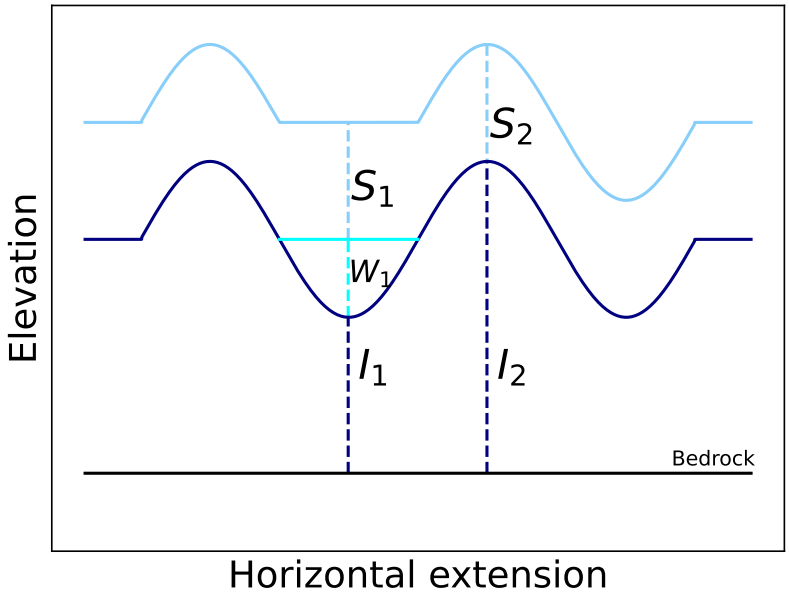


**Figure 2.** Instances of Greenland profile, we see the ice thickness $I$ (dark blue), the water thickness $W$ (cyan) and the snow $S$ (light blue). We remark that the snow thickness is constant in our model, therefore in particular $S_1 = S_2$.

### 2.1 Ice equation

To model the Greenland Ice Sheet, we use a modified version of the ice profile models based on the shallow-ice approximation (Greve and Blatter, 2009). This model is a simplified version of the Stokes' flow, considering that the width of the ice sheet resting on a flat bedrock is significantly larger than its thickness. We assume that there is no basal melting or sliding, and the ice possesses a constant viscosity. The ice equation, similar to the one used in (Klose et al., 2024) reads:

$$\frac{\partial I}{\partial t} = \begin{cases} 0 & \text{if } I = 0^*, \\ \frac{\partial}{\partial x}\left(\frac{2A(\rho_{\text{ice}}g)^n}{n+2}\left|\frac{\partial I}{\partial x}\right|^{n-1}\frac{\partial I}{\partial x}I^{n+2}\right) - (T - T_0)\text{MRI}(W) + \text{L}_H\Delta I & \text{if } I > 0, T \geq T_0 \text{ and } S = 0^*, \\ \frac{\partial}{\partial x}\left(\frac{2A(\rho_{\text{ice}}g)^n}{n+2}\left|\frac{\partial I}{\partial x}\right|^{n-1}\frac{\partial I}{\partial x}I^{n+2}\right) + \text{L}_H\Delta I & \text{otherwise.} \end{cases} \tag{1}$$

and the conditions marked with $*$, indicate that during computations these quantities can be negative within integration algorithm tolerance. Our equations describe two main phases of the ice thickness evolution: the melt regime, characterized by positive temperatures and lack of snow which results in the transformation of bare ice into water, and the non-melt regime, where only mechanical processes take place.

In the right-hand sides of Eq. 1, the first term of the equations describes the divergence of the ice flux, $MRI$ describes the melt rate of the ice and $L_H\Delta I$ is a diffusion process in the form of a Laplacian, it acts as a stabilization term that can be

https://doi.org/10.5194/egusphere-2025-6334
Preprint. Discussion started: 20 January 2026
© Author(s) 2026. CC BY 4.0 License.

interpreted as the small scale spatial variation of the ice surface. The parameter $A$, is an Arrhenius factor that quantifies how easily ice deforms for a given temperature, $n$ is the exponent of Glen's Flow Law, an empirical creep relation (Glen, 1952), $\rho_{\text{ice}}$ is the density of ice and $g$ is the gravitational acceleration.

The melt rate of ice $MRI$ plays a fundamental role in the process of the formation of supraglacial lakes. Here we distinguish between the melt rate of bare ice and the melt rate which occurs if the ice is covered with a supraglacial lake. At locations with no supraglacial lakes, the melt rate takes the value $m_{\text{I}}$ of bare ice, while at locations with a supraglacial lake, the melt rate takes values up to $m_l$. If the ice sheet is covered with snow, no melting of ice takes place, which is indicated by the second equation in Eq. 1. All molten ice thickness is converted immediately to water, increasing the value of $W$. When the ice surface is covered by snow, melting initially occurs exclusively in the snow layer at a rate $m_{\text{S}}$; only after the snow is completely depleted the underlying ice profile can start melting. The values of the melt rates we use are typical values for the positive degree days (PDD) scheme (Reeh, 1989; Braithwaite, 1995; Zhang et al., 2006), a simple empirical yet powerful method for estimating the melt rate of snow and ice when temperatures are above the critical temperature $T_0 = 0\,°C$ (Cuffey and Paterson, 2010). This estimation is based on considering the melt rate to be proportional to positive temperature, i.e. assuming a melt rate that increases proportionally to $T - T_0$ multiplied by a constant factor that represents the surface material properties with the unit m $s^{-1}$ $°C^{-1}$. The melting process following the PDD scheme leads to the formation of water, taking into account that the presence of supraglacial lakes accelerates the process of melting because of the higher albedo of the supraglacial lakes. Observations of melt rates at supraglacial lakes found that melt rates of the corresponding ice beneath the water are approximately twice the melt rate of bare ice (Tedesco et al., 2012), for this reason, we consider $m_l = 2m_{\text{I}}$. For a snow-free surface, the $MRI$ function determines the melt rate of ice using a linear interpolation between the melt rates for bare ice, $m_{\text{I}}$, and for a fully developed supraglacial lake, $m_l$. The albedo of bare ice is given by $\alpha_0 = \alpha(W = 0) \approx 0.55$. For an infinitely deep supraglacial lake, where the albedo approaches $\alpha_l = \lim_{W\to\infty} \alpha(W) = 1/20$, the melt rate is assumed to be twice the PDD melt rate. Intermediate melt rates are computed using linear interpolation between these two cases, depending on the water thickness at each location.

$$\text{MRI}(W) = \frac{(\alpha(W) - \alpha_l)(m_{\text{I}} - m_l)}{\alpha_0 - \alpha_l} + m_l \tag{2}$$

The equation we use for the albedo of the supraglacial lakes $\alpha(W)$ is taken from Lüthje et al. (2006b), and describes the dimensionless decreasing albedo depending on the thickness of the lakes W. The albedo plays a key role in the feedback loop, as it accounts for the increasing absorbed radiation and meltrate observed in lakes with larger water thickness:

$$\alpha(W) = \frac{9702 + 1000e^{3.6W}}{-539 + 20000e^{3.6W}}. \tag{3}$$

Finally, the Laplacian operator with coefficient $L_H$ as the third term of Eq. 1 is introduced to numerically stabilize the evolution of the ice thickness (dos Santos et al., 2021).

https://doi.org/10.5194/egusphere-2025-6334
Preprint. Discussion started: 20 January 2026
© Author(s) 2026. CC BY 4.0 License.

## 2.2 Water equation

The water equation accounts for two distinct processes: surface melting, which forms supraglacial lakes, and drainage through seepage, which removes water from the surface; the latter is illustrated in Fig. 1b.

$$\frac{\partial W}{\partial t} = \begin{cases} m_{\mathrm{S}}(T - T_0)\frac{\rho_{\mathrm{snow}}}{\rho_{\mathrm{water}}} - \mathrm{SE}(W) & \text{if } T \geq T_0 \text{ and } S > 0, \\ \mathrm{MRI}(W)(T - T_0)\frac{\rho_{\mathrm{ice}}}{\rho_{\mathrm{water}}} - \mathrm{SE}(W) & \text{if } T \geq T_0 \text{ and } S = 0^*, \\ -SE(W)\Theta(W) & \text{otherwise} \end{cases} \tag{4}$$

The melting process depends on the ice coverage by snow and the temperature. As long as snow covers the ice surface, only the snow melts when temperatures become positive, as reflected in the first Eq. of Eqs 4. When all snow is gone, the melting of the bare ice starts at the rate $MRI$ described earlier. The seepage $SE$ refers to the infiltration or percolation of liquid water as it moves vertically through the porous structure of the ice. As the ice melts and water accumulates on the surface, it can percolate vertically into the ice sheet through fine fractures, potentially reaching lower layers of ice or finally even the bedrock beneath the ice sheet, or it can abruptly drain when it reaches a predefined water thickness $W_{\mathrm{drain}}$ or temperature $T_{\mathrm{rem}}$. In our model, once water leaves the surface through seepage or abrupt removal, it is considered permanently removed and is no longer included in subsequent integration steps. In our equation, we use the Heaviside function to indicate that seepage is the only relevant process during the cold period, provided water is still present.

$$\Theta(x) = \begin{cases} 0 & \text{if } x \leq 0, \\ 1 & \text{if } x > 0, \end{cases} \tag{5}$$

The loss of water is described by the seepage rate function $SE$. Seepage is a crucial phenomenon in this study because it governs how meltwater is removed as it penetrates deeper layers of the ice and eventually reaches the bedrock. However, the details of this process are not well understood so far. For sea ice melt ponds, the mechanism driving seepage considers the porous structure of sea ice and follows Darcy's law (Scott and Feltham, 2010; Scagliarini et al., 2020), with the value of the seepage proportional to the ratio between water and ice thickness. In contrast to Lüthje et al. (2006b), where the seepage rate is constant, we consider it to depend linearly on the water thickness multiplied by a rate $s_r$. This approach reflects the idea that the seepage is proportional to the pressure that the water column exerts on the ice profile, as suggested by Stevin's law; however, a more rigorous approach would require a unit-adjusting constant, so we simply refer to $s_r$ as the seepage rate.

$$\mathrm{SE}(W) = s_r W \tag{6}$$

While the consideration of melting and seepage processes are similar to the ones suggested by Lüthje et al.(Lüthje et al., 2006a, b), we use a different approach to take into account the movement of the water on the ice surface. Since the ice surface is not flat, the formation of supraglacial lakes depends crucially on the flow of water towards the valleys in the ice thickness

https://doi.org/10.5194/egusphere-2025-6334
Preprint. Discussion started: 20 January 2026
© Author(s) 2026. CC BY 4.0 License.

profile $I$. In contrast to Lüthje et al. (2006a, b) we use a simplified mass conservative algorithm consisting of steps to move the water instantaneously after melting and seepage to form a flat water surface within the valleys of the ice profile. Here, our algorithm is less sophisticated compared to many approaches used in the literature, e.g. Banwell et al. (2012), Mohanty and Maiti (2022), since we restrict ourselves to a two-dimensional vertical cross-section through the ice sheet. The water flow is managed by an algorithm that is called frequently after integration steps, in particular we call it after every second time step. In this algorithm we assume that any two consecutive maxima in the ice profile define the presence of a supraglacial lake. The content of water for all grid cells in such a supraglacial lake is redistributed to form a flat water surface. If the amount of water coming from the melting process does not fit into the lake it will overflow to the next available lake. Most of the computations are done basin by basin and not pointwise, allowing a fast execution time.

**Algorithm 1** Water flow

**Require:** Variables: $I$, $W$; Tolerance thresholds: $T_a$, $T_b$
  Find relative maxima in $I$ and assign$\rightarrow M$
  $\forall$ basins, compute capacity and water contained
  **while** Merging still in progress AND maximal overflow in $M > T_a$ **do**
    **for** each relative maximum $m$ left in $M$ **do**
      remove one $m$ that has neighboring basins that overflow into each other.
      $\forall$ basins, compute capacity and water contained
    **end for**
    **for** each $m$ in $M$ **do**
      Move $50\%$ of eventual overflowing water left or right, depending on the lowest margin in the basin.
      $\forall$ remaining basins, compute capacity and water contained
    **end for**
  **end while**
  **for** each basin $p$ left **do**
    Calculate the water amount in each basin $p$ within tolerance $T_b$
    Assign the new water value to each point in $W$
  **end for**
  **return** $W$

The algorithm requires an initial configuration of the surface of the ice sheet and the water distribution, both specified grid cell by grid cell, to ensure accurate water flow behavior. As a first step, it identifies the local maxima within the horizontally periodic domain. In cases where a plateau exists, i.e. neighboring points share the same thickness value, the algorithm selects the central point of the plateau, rounding the index down. Each identified maximum is then associated with a corresponding basin, specifically the one located immediately to its right. This strategy allows for a fast execution time because the algorithm operates with the properties of the basin and not with a point-by-point computation, which requires longer and costlier loops.

https://doi.org/10.5194/egusphere-2025-6334
Preprint. Discussion started: 20 January 2026
© Author(s) 2026. CC BY 4.0 License.

For each basin we use three main quantities in the algorithm: the amount of water that the basin contains, the maximum amount of water that the basin might contain without overflowing and the lowest boundary (which is a relative maximum) of the basin.

The water distribution takes place in a loop where two main actions are performed continuously:

1. Two basins are merged if they overflow into each other, with the evaluation being made with the amount of water contained in each basin as well as the maximum amount a basin could contain. If there is only one basin left, no further merging actions are performed.

2. Half of the overflowing water in one basin is moved toward a neighboring basin, considered according to the lowest boundary of the basin (if the basin has two equally high neighboring margins, the water is split equally between the two)

We repeat the two actions until no more basins are merging and the overflowing water is smaller than the threshold $T_a$.

The algorithm is mass-conserving, as it only contemplates movement of water, furthermore the water movement stops because the overflow reaches the tolerance threshold ($T_a$) or all the basins are merged into one.

To determine the water thickness at each point within a basin, we use an iterative approach inspired by the bisection method that uses a second tolerance threshold $T_b$. We start by choosing a lower and an upper bound for the possible water thickness. For each trial thickness (the midpoint between the bounds), we calculate the total water volume that would result. If this volume is greater than the target volume, we lower the upper bound; if it is less, we raise the lower bound. By repeatedly updating the bounds in this way, the interval narrows until the estimated water thickness converges to a value within $T_b$, producing the desired total volume in the basin.

### 2.3 Snow equation

Snow accumulation and melt processes are governed by temperature. When the temperature is below a threshold temperature $T_0 = 0$ °C, the model assumes that the snow accumulates at a constant rate $S_{\text{ar}}$ without melting. If $T \geq T_0$, the snow melts according to the PDD scheme. The snow that is lost due to melting is added to the water equation.

$$\frac{\partial S}{\partial t} = \begin{cases} -m_{\text{S}}(T - T_0)\Theta(S) & \text{if } T \geq T_0 \\ S_{\text{ar}} & \text{if } T < T_0 \end{cases} \tag{7}$$

The Positive Degree Days (PDD) scheme we employ, assumes that ice and snow are at their melting point when $T > T_0$. For simplicity, we treat snow and water as distinct phases and neglect slush formation. Although the presence of slush or water-saturated snow would influence energy absorption and feedback processes, such interactions are not compatible with the positive degree-day approach, which assumes that ice and water remain at the melt temperature.

Furthermore, we assume that there is no horizontal flow of snow in our model, i.e. snow does not move laterally across the surface. Therefore, transport terms for snow are neglected. By doing this, we can focus on the melting effects only. The water equivalent snow accumulation rates used in our model are lower than those reported by RACMO ($0.44 \pm 0.08$ m a$^{-1}$) and MAR ($0.37 \pm 0.09$ m a$^{-1}$) models for western coastal zones (Machguth et al., 2024). This choice is intentional, as we aim to

https://doi.org/10.5194/egusphere-2025-6334
Preprint. Discussion started: 20 January 2026
© Author(s) 2026. CC BY 4.0 License.

isolate and analyze a feedback mechanism driven by the continuous melting of snow and subsequent formation of supraglacial lakes, whilst these processes do not emerge under higher accumulation conditions.

### 2.4 Temperature forcing

Understanding the surface temperature variability over the GrIS is a fundamental aspect to achieve a reasonable representation of melt processes and their seasonal dependence. We model the yearly atmospheric temperature at the ice surface by a cosine function that is modified to match the mean annual and July temperature at a given location. Our temperature equation is based on the positive-degree day (PDD) scheme in (Reeh, 1989; Marshall and Sharp, 2009), however, instead of having parameters that describe the temperature for a given latitude, we remove the corresponding term in the empirical scheme. We simplify the parametrization by considering an initial location in Greenland corresponding to the KAN-L base in the K-transect (Smeets et al., 2018), using the corresponding initial mean yearly and July temperatures $TMA_{init}$ and $TMJ_{init}$ and initial elevation $I_{init}$. Our formula now depends only on the elevation of the profile, where in particular, the initial elevation corresponds to the measured temperature, while future temperatures are influenced by the melt elevation and described by the formulas:

$$TMA(S,I,W) = TMA_{init} + c_{me}[\text{mean}(S+I+W) - I_{init}] \tag{8}$$

$$TMJ(S,I,W) = TMJ_{init} + c_{me}[\text{mean}(S+I+W) - I_{init}] \tag{9}$$

The thickness of the ice profile $I$ introduces a simple linear relationship between elevation and temperature (Levermann and Winkelmann, 2016) by the coefficient $c_{me}$ that causes a temperature increase of circa $8\ ^{\circ}C$ for each kilometer drop in ice thickness. We obtain the seasonal parametrization for $T$ by using the long-term mean July air temperature *TMJ*:

$$T = TMA(S,I,W) + (TMJ(S,I,W) - TMA(S,I,W))\cos(2\pi t/s_y + \gamma) \tag{10}$$

Where $\gamma$ is the phase of the cosine, chosen such that the simulation starts at the end of the melting season during the first simulation year. In our model, we select parameters that approximately match those of the KAN-L station in Greenland. Although more complex and physically based approaches exist to describe ice and snow melt in Greenland (Pollard, 1980; van den Berg et al., 2008; Tsai and Ruan, 2018), we focus on the simpler energy balance method to highlight the essential mechanisms driving surface melt.

### 2.5 Implementation

In our model, we simulate a 2D slice of the Greenland Ice Sheet spanning 40 km. The initial ice thickness $I$ is set to the current value of ice thickness plus random noise, and then we allow the ice profile to evolve over a spin-up period using the equation below to develop a reasonable landscape:

$$\frac{\partial I}{\partial t} = \frac{\partial}{\partial x}\left(\frac{2A(\rho_{\text{ice}}g)^n}{n+2}\left|\frac{\partial I}{\partial x}\right|^{n-1}\frac{\partial I}{\partial x}H^{n+2}\right) + L_H\Delta I \tag{11}$$

https://doi.org/10.5194/egusphere-2025-6334
Preprint. Discussion started: 20 January 2026
© Author(s) 2026. CC BY 4.0 License.

We initialize the snow field to contain no snow at the start, and likewise, we initialize the water thickness with no water.

Our integration scheme is based on the *solve_ivp* python package, where we use the LSODA integrator to mathematically integrate the three coupled equations. To numerically solve the partial differential equations, we discretize the spatial domain using a uniform grid with spacing $\Delta x$. Derivatives (gradient and Laplacian) with respect to $x$ are approximated using fourth-order finite difference (FD) schemes as follows:

Gradient:

$$\left.\frac{\partial Z}{\partial x}\right|_i \approx \frac{-Z_{i+2} + 8Z_{i+1} - 8Z_{i-1} + Z_{i-2}}{12\,\Delta x}. \tag{12}$$

Laplacian:

$$\left.\frac{\partial^2 Z}{\partial x^2}\right|_i \approx \frac{-Z_{i+2} + 16Z_{i+1} - 30Z_i + 16Z_{i-1} - Z_{i-2}}{12\,\Delta x^2}. \tag{13}$$

These finite difference approximations are substituted into the PDE to obtain a system of ordinary differential equations suitable for numerical computation. We apply periodic boundary conditions, which guarantee that the leftmost point in the domain coincides with the rightmost one, creating a *wrap-around* effect. Periodic boundary conditions are used to mimic a longer spatial domain than the 40 km considered. This is a usual technique in studying PDEs.

We set up the model in such a way that the first simulated year begins at the start of the cooling phase of the temperature cycle, i.e., when the temperature first drops below zero at the initial thickness. If the cycle does not include negative temperatures, we instead define the initial phase of the cosine function as zero. This choice avoids the need to guess an initial snow amount, which is difficult to estimate and could otherwise create unrealistic transient effects at the beginning of the simulation.

The main parameters used in the equations are listed in Table 1, while additional parameters and variables are provided in Table A1 in the appendix (Section A).

## 3 Evolution of ice thickness

Let us now investigate the evolution of the ice thickness when the formation of supraglacial lakes is taken into account. We integrate the model described above over 200 years with additional 10 years of spin-up using the parameter set in Table 1. The results for the simulation run are shown in Fig. 3 for the yearly means of ice thickness ($A$), water thickness ($B$), snow thickness ($C$), temperature ($D$). Additionally, we show the yearly mean of the water runoff ($E$). For better visualization of the impact of supraglacial lakes, we compare our simulations to computations (in blue) without lake formation (in black).

We observe that temperature increases as a result of decreased ice surface. This rise in temperature has a cascading effect on all the main variables in the system. Ice thickness decreases in both simulations, but the scenario including supraglacial lakes shows a more rapid loss of ice. This amounts to a thickness difference of circa 90 meters at the end of the simulation. Regarding water storage, the mean behavior is irregular but shows an overall decreasing trend. This can be attributed to increased melting at lower elevations (due to higher temperatures), causing lakes to drain more rapidly and intermittently reset the accumulation process. Despite of this, water runoff continues to increase over time and accelerates in both scenarios (with and without lakes).

https://doi.org/10.5194/egusphere-2025-6334
Preprint. Discussion started: 20 January 2026
© Author(s) 2026. CC BY 4.0 License.

**Table 1.** Model parameters and their corresponding variable names in the code, values, units, and short descriptions. For clarity, we split the table into four categories: Physical Constants, Thermal Parameters, Melt and Accumulation, and Ice Flow Dynamics.

| Variable | Variable (code) | Value | Unit | Explanation |
|---|---|---|---|---|
| $g$ | g | 9.81 | m $s^{-2}$ | Gravitational acceleration |
| $\rho_{\text{ice}}$ | rho_ice | 917 | kg $m^{-3}$ | Ice density |
| $\rho_{\text{snow}}$ | rho_snow | 350 | kg $m^{-3}$ | Snow density |
| $\rho_{\text{water}}$ | rho_water | 1000 | kg $m^{-3}$ | Water density |
| $TMA_{init}$ | TMA_init | -12.5 | °C | Initial mean annual temperature |
| $TMJ_{init}$ | TMJ_init | 4 | °C | Initial mean July temperature |
| $T_0$ | T_0 | 0 | °C | Melting point |
| $T_{\text{rem}}$ | T_rem | -5 | °C | Removal temperature for meltwater |
| $c_{\text{me}}$ | c_me | -0.007924 | °C $m^{-1}$ | Melt-elevation rate |
| $m_l$ | m_rate_p | 16 | mm $day^{-1}$ $°C^{-1}$ | Melt rate (limit value with lakes) |
| $m_{\text{S}}$ | m_rate_s | 3 | mm $day^{-1}$ $°C^{-1}$ | Melt rate (snow) |
| $m_{\text{I}}$ | m_rate_i | 8 | mm $day^{-1}$ $°C^{-1}$ | Melt rate (bare ice) |
| $S_{\text{ar}}$ | S_ar | 0.15 | m $a^{-1}$ | Snow accumulation rate (water eq.) |
| $s_r$ | s_r | 0.6 | mm $day^{-1}$ $m^{-1}$ | Seepage rate |
| $W_{\text{drain}}$ | W_drain | 5 | m | Water thickness at which lakes drain instantaneously |
| $A$ | A | $10^{-16}$ | $a^{-1}$ $Pa^{-3}$ | Glen's flow rate factor |
| $n$ | n | 3 | - | Glen's flow exponent |
| $L_H$ | L_H | 0.0001 | $s^{-2}$ | Diffusion in ice equation |

Snow thickness also declines as elevated temperatures reduce the number of days with negative temperatures (therefore limiting snow accumulation). This effect is further amplified in the presence of supraglacial lakes (which enhance surface melting).

As previously mentioned, the melting of the ice is significantly more pronounced in scenarios with supraglacial lakes, as illustrated in Figures 4 and 5. The ice thickness profiles clearly demonstrate that the presence of supraglacial lakes drastically alters the lake-ice sheet landscape. When supraglacial lakes are not considered, the evolution is mainly driven by diffusion and melting, resulting in a gradual lowering and flattening of the ice surface. However, when supraglacial lakes are present, their basins dominate the landscape due to the positive feedback loop caused by increased absorption of radiation.

In the ice profile specifically, the initial thickness difference between maxima and minima is approximately 5 meters. In the scenario without water, this difference decreases to about one meter over time, whereas in the presence of supraglacial lakes, it amplifies dramatically to around 50 meters. This occurs because water tends to accumulate repeatedly in the same depressions formed by lakes in previous years making them deeper.

https://doi.org/10.5194/egusphere-2025-6334
Preprint. Discussion started: 20 January 2026
© Author(s) 2026. CC BY 4.0 License.

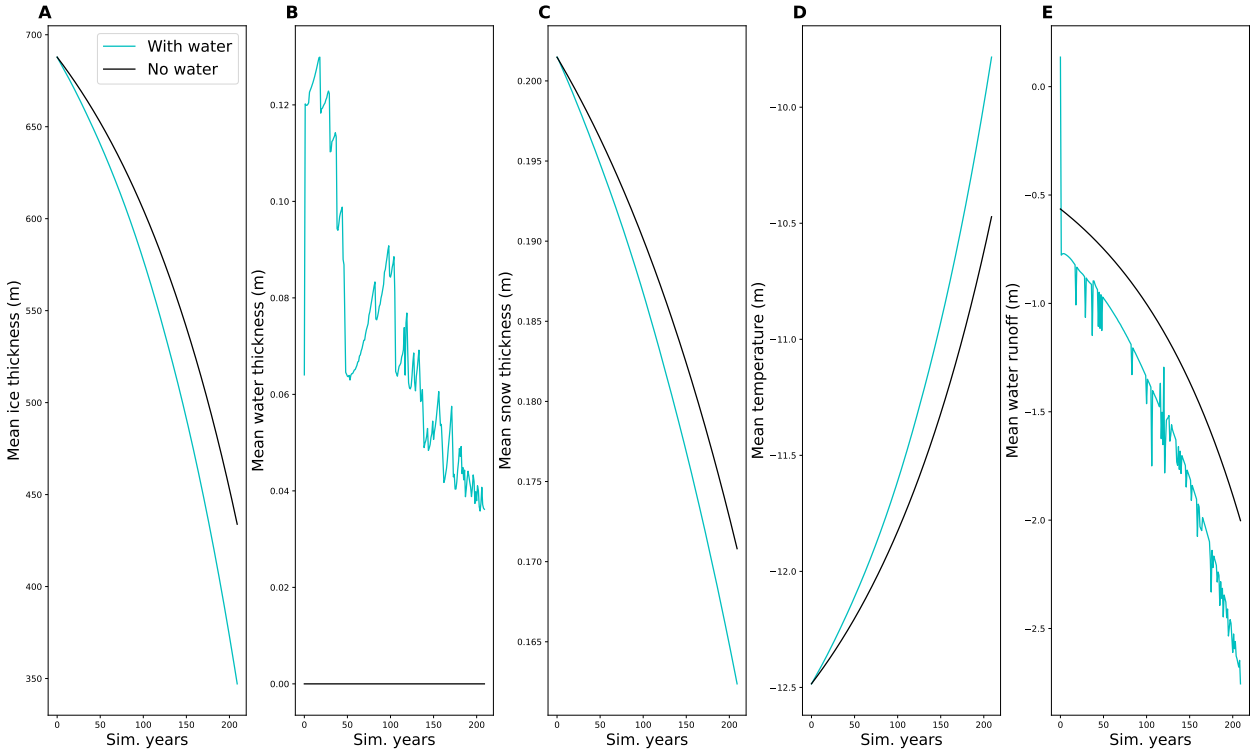


**Figure 3. Variable means in simulation.**. We show the year means of ice thickness (panel A), water thickness (B), snow thickness (C), mean temperature (D) and mean water runoff (E) for a simulation time of 210 yrs, including 10 of spin-up. The cyan lines indicate the experiments with supraglacial lakes, while the black ones the experiments without.

The water thickness profile shown in Figure 4 (panel C) reveals interesting dynamics. When the ice surface is shallow, lakes easily merge, leading to significant ice melting and becoming confined by the basin boundaries. Initially, lakes are wider, but as they deepen and form more pronounced basins, they become narrower. Despite their reduced surface area, these deeper basins collect more water and therefore drain more rapidly.

## 4 Sensitivity analysis of the model

Our model includes several parameters whose values are not precisely known from observations; hence, they must be prescribed based on plausibility considerations. However, our results depend on those parameters, and a sensitivity analysis can help to understand the extent to which results change when changing those parameters. We vary each parameter $p$ over an interval $[\frac{1}{2}p, 2p]$, where $p$ is the prescribed value of the parameter used in this study. To better assess their influence on the model, we analyze how each parameter affects the model simulations, with a particular focus on the evolution of the ice thickness profile. For each parameter, we perform experiments under two conditions: one that includes the effects of surface water (supraglacial lakes and meltwater feedbacks), and one that excludes them. This allows us to isolate and compare the role of each parameter

https://doi.org/10.5194/egusphere-2025-6334
Preprint. Discussion started: 20 January 2026
© Author(s) 2026. CC BY 4.0 License.

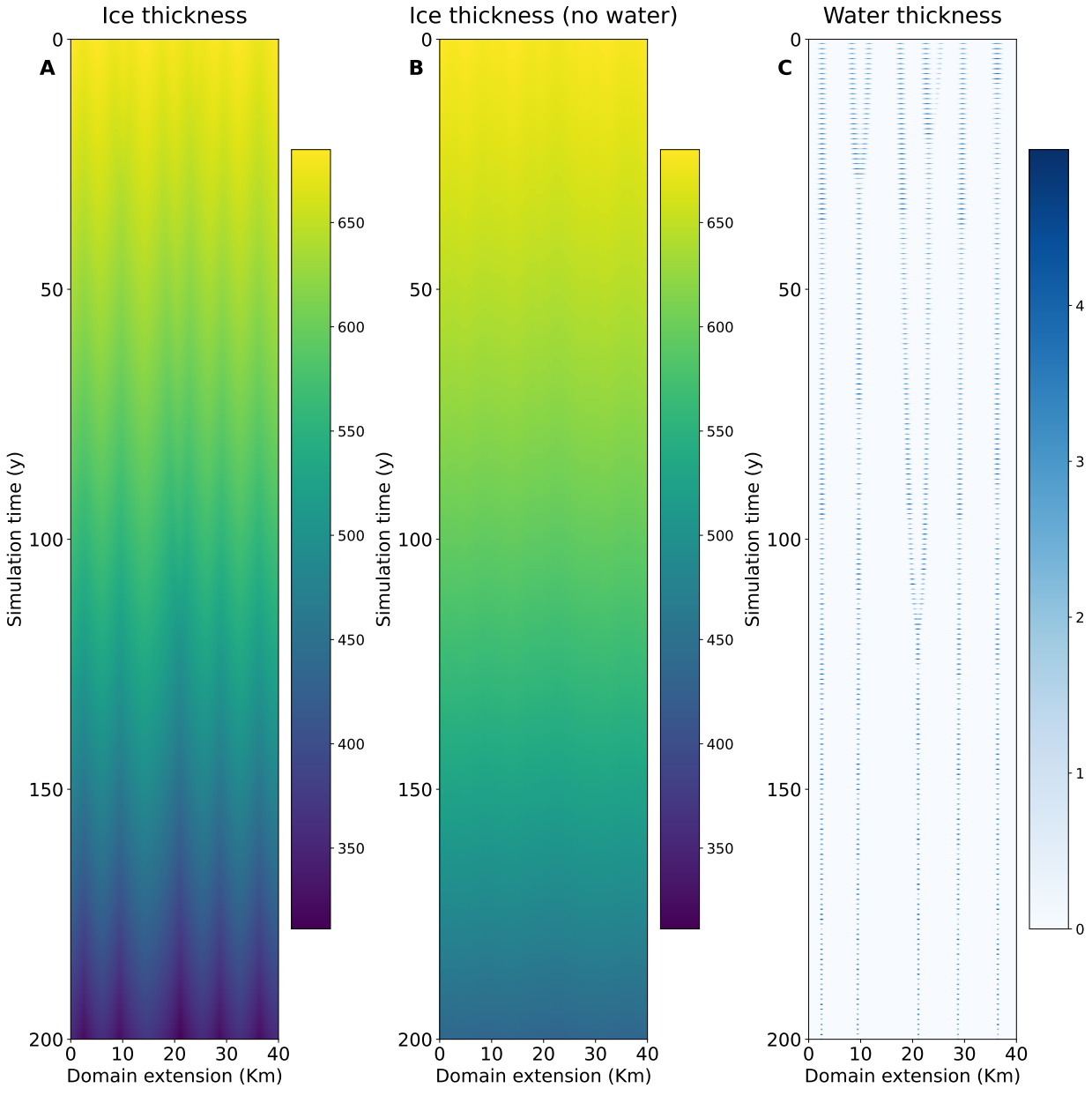


**Figure 4. Ice thickness and water for 200 yrs of simulation** Panels A and B illustrate the ice thickness profiles over the course of a complete simulation run. Panel A specifically highlights the evolution of ice thickness with the influence of supraglacial lakes, while Panel B presents the scenario without the presence of supraglacial lakes. Panel C displays the water thickness evolution throughout the simulation period.

in both hydrologically active and inactive scenarios, providing a clearer understanding of their contributions to ice dynamics

https://doi.org/10.5194/egusphere-2025-6334
Preprint. Discussion started: 20 January 2026
© Author(s) 2026. CC BY 4.0 License.

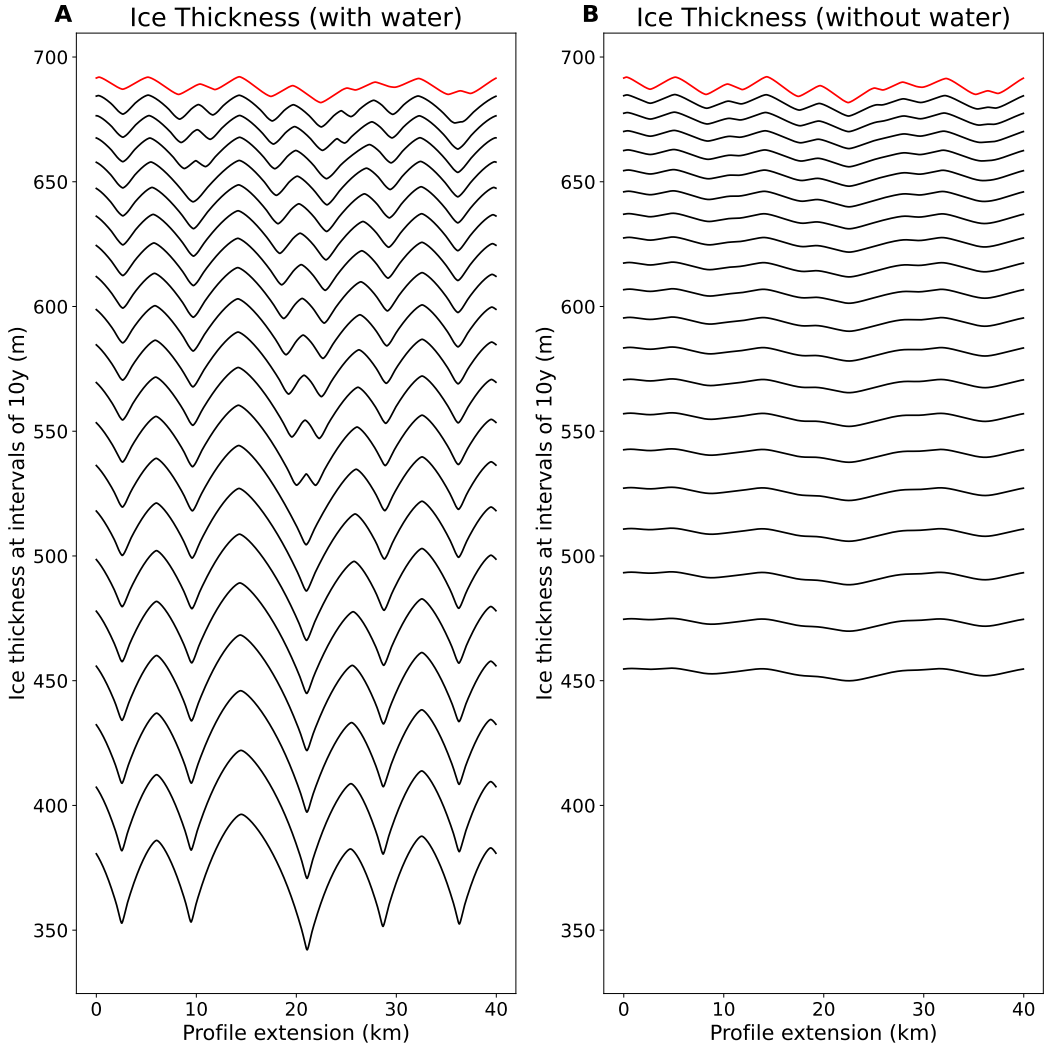


**Figure 5. Time instances for ice profile** We plot the initial ice profile in red and then show profiles every 10th year in black. Panel A displays the ice profile with supraglacial lakes, while Panel B shows the profile without supraglacial lakes.

and melt behavior. The results of these tests are summarized in Figure 6 and the effect of each variable change is described below.

https://doi.org/10.5194/egusphere-2025-6334
Preprint. Discussion started: 20 January 2026
© Author(s) 2026. CC BY 4.0 License.

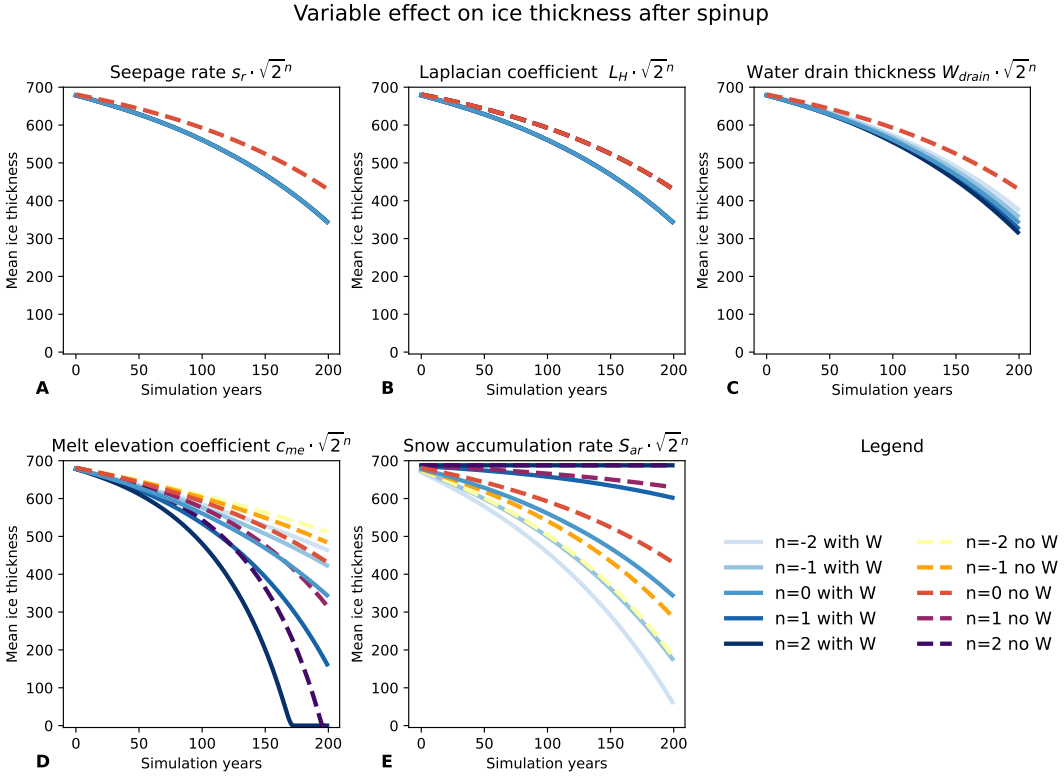


**Figure 6. Parameter sensitivity evaluation**. Each of the subplots show the sensitivity analysis for each of the parameters $s_r$ (A), $L_H$ (B), $W_{\text{drain}}$ (C), $c_{\text{me}}$ (D), $S_{\text{ar}}$ (E). Each line in the plots shows the ice thickness for a single variable change multiplied by $\sqrt{2}^n$ for n $\in \{-2, -1, 0, 1, 2\}$ so that, among other possibilities, we both double and half the variable. The case $n = 0$ corresponds to the original model. We perform these tests for both models with and without effect of supraglacial lakes.

– **Seepage rate** $s_r$ modification has no relevant effect on the model results in the considered range. Even though higher seepage rates yield shallower supraglacial lakes, the albedo of the lakes is only slightly smaller for the shallower ones. If we consider the different scenarios with water, we observe that the difference in ice thickness at the end of the simulations is of the order of a few centimeters. Additionally, for the scenarios without supraglacial lakes, the parameter does not affect the model at all because no water penetrates through the ice dome.

– **Laplacian coefficient** $L_H$ variation causes differences on the order of magnitude of centimeters without water, and on the order of magnitude of tens of centimeters with water (at the end of the simulation considered). Higher values of the parameter $L_H$ lead to more melting. This happens because the parameter governs lateral smoothing processes and tends to make the ice thickness profile flatter due to the effect of diffusion. This flatness accelerates melting due to the fact that

https://doi.org/10.5194/egusphere-2025-6334
Preprint. Discussion started: 20 January 2026
© Author(s) 2026. CC BY 4.0 License.

formed supraglacial lakes are wider and can melt more water. However, this effect can hardly be seen for the different scenarios because of the scale of the figures.

- **Water drainage thickness** $W_{drain}$ has a visible effect on the evolution of the ice thickness. Although it does not affect the scenario if supraglacial lakes are not present, drainage thickness $W_{drain}$ leads to an increased radiative feedback because the water stays for longer in the lake and absorbs more radiation. If the water drains more quickly, the feedback mechanism is suppressed, and the surface becomes ice-free more often. As a result, the difference between the final states of the scenarios is on the order of several tens of meters.

- **Melt elevation coefficient** $c_{me}$ has a large effect on the model. For both scenarios considered, we clearly see that doubling this parameter causes the complete melting of the ice profile in less than 200 years of integration. The melt elevation coefficient can largely amplify the melting of ice by altering the temperature through the melt-elevation feedback: as the ice thickness profile becomes lower, the temperature increases, leading to higher melt rates and less snow, resulting in accelerated ice loss. Reducing the parameter value still leads to accelerating melt scenarios, but the ice is lost more slowly.

- **Snow accumulation rate** $S_{ar}$ has a large effect on the ice evolution. If we increase the snow accumulation rate, we have a scenario where, although the snow melts, the accumulation is larger, thus preventing the ice profile surface from being exposed to the atmosphere. Therefore, whether or not we have water in the system, snow continues to accumulate on top. Conversely, decreasing the amount of snow that falls in a year leads to a feedback with the opposite sign, where faster ice melting due to higher coefficients in the PDD scheme prevails. This effect is amplified by the lowering of the surface profile: as the ice becomes thinner, snow accumulation decreases further. The reduced snow cover accelerates ice loss, which is especially pronounced in the scenario with supraglacial lake amplification, leading to substantial ice loss over the 200-year simulation.

## 5 The impact of global warming scenarios

We test our model using global mean temperatures from comprehensive earth system models CESM2 and NorESM2 (Norwegian Climate Centre, 2019; NCAR, 2020), under several future Shared Socioeconomic Pathways (SSP) scenarios: SSP1-2.6, SSP2-4.5, SSP3-7.0, and SSP5-8.5 (O'Neill et al., 2016), which span a range from strong climate mitigation to high-emission (business as usual) scenarios (cf. Fig. 7). To implement the temperature changes in the model, we modify the formulation of the mean annual temperature and mean July temperature, as described in Equations 14 and 15.

$$TMA(i,S,I,W) = TMA_i + c_{me}[\text{mean}(S+I+W) - I_{\text{init}}] + C_{\text{my}}(GMT_i - GMT_1), \tag{14}$$

$$TMJ(i,S,I,W) = TMJ_i + c_{me}[\text{mean}(S+I+W) - I_{\text{init}}] + C_{\text{mj}}(GMT_i - GMT_1), \tag{15}$$

https://doi.org/10.5194/egusphere-2025-6334
Preprint. Discussion started: 20 January 2026
© Author(s) 2026. CC BY 4.0 License.

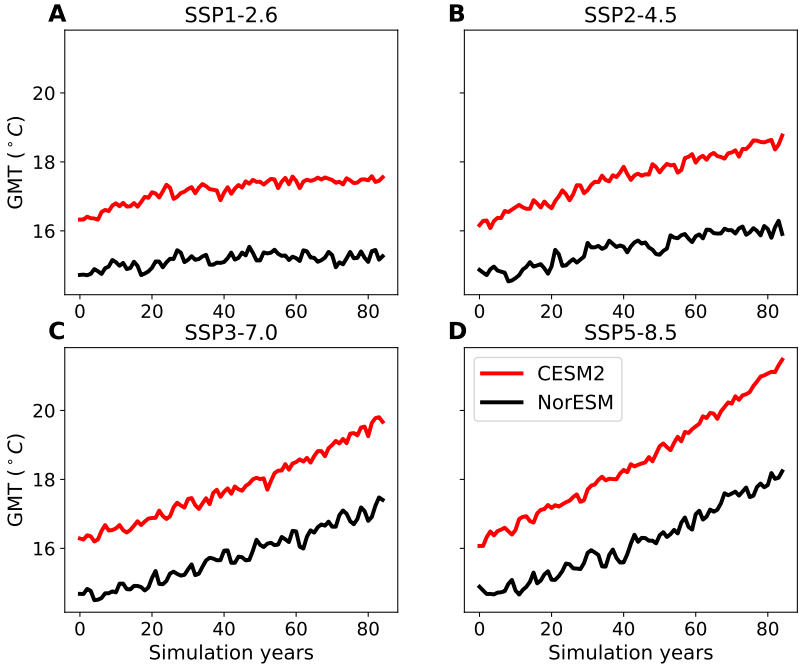


**Figure 7. Global mean temperatures for different models and scenarios.** Both the models' outputs used (CESM2 and NorESM) are shown, together with all scenarios used (A to D).

where $GMT_i$ is the yearly global temperature mean taken from the output of the two climate models CESM2 and NorESM (see Figure 7), $C_{\mathrm{my}} = 3$ and $C_{\mathrm{mj}} = 1.5$ are dimensionless constants indicating Arctic amplification for mean temperature and mean July temperatures in the Arctic, compatible with the results in Rantanen et al. (2022). Additionally, we test all scenarios both with and without the presence of supraglacial lakes in the model, and under different snow accumulation rates (specifically, $S_{\mathrm{ar}} = 0.15$ m a$^{-1}$ , $S_{\mathrm{ar}} = 0.25$ m a$^{-1}$ and $S_{\mathrm{ar}} = 0.35$ m a$^{-1}$ , with the latter being close to MAR model output, see (Machguth et al., 2024). The results are shown in Fig. 8.

We see from Figure 8 that in general CESM2 enhances the melting of ice compared to NorESM. Snow accumulation is a crucial factor, as previously discussed (models with low snow accumulation have ice that is less protected from solar radiation and tends to melt faster), as already described in the melt-albedo feedback (Box et al., 2012). As expected, all the warmer scenarios correspond to faster melting. In particular, in cases of increased snow accumulation, snow initially accumulates on top of the ice profile, then as temperatures increase, the snow melts, uncovering the ice underneath for longer periods of time and starting the melting loop. The scenarios with higher snow accumulation (which is closer to actual conditions, panels C and F in Figure 8) have the melting loop starting later for the scenarios with higher emissions (SSP 5 8.5), indicating that in

https://doi.org/10.5194/egusphere-2025-6334
Preprint. Discussion started: 20 January 2026
© Author(s) 2026. CC BY 4.0 License.

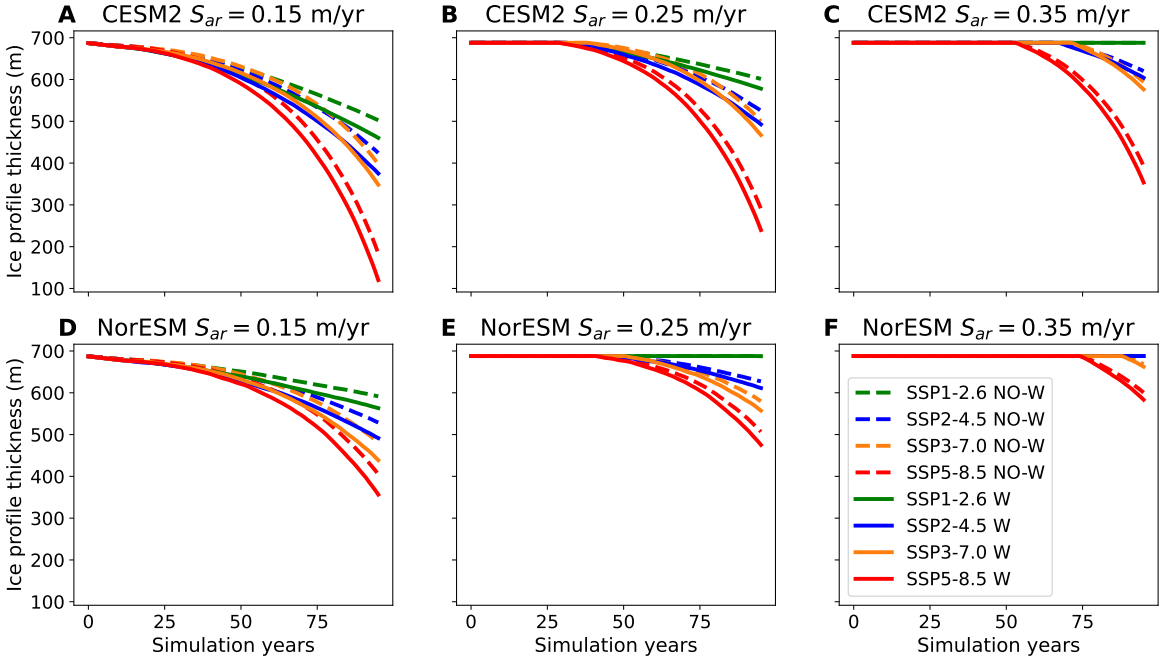


**Figure 8. Ice thickness for different warming scenarios** Each panel shows the time evolution (2015–2100) of the mean sea ice thickness over the domain. Continuous lines represent scenarios without water and without supraglacial lakes, while dashed lines represent scenarios without water only. Panels A and D, B and E, and C and F correspond to increasing snow accumulation rates. The upper panels are forced by CESM2 model output, while the lower panels use NorESM output.

real conditions this melting loop may begin as soon as in 2065 (CESM2) or 2090 (NorESM). These comparisons highlight the combined influence of climate forcing, hydrology, and snow accumulation on sea ice evolution throughout the 21st century.

## 6 Conclusions

The formation of supraglacial lakes can accelerate melting of the Greenland Ice Sheet, particularly in regions like western Greenland where climatic conditions favor their development. By reducing the surface albedo, these lakes increase the absorption of solar energy, enhancing local surface melt rates and contributing to a positive feedback loop that amplifies ice loss.

Our simplified model reproduces the relevant interactions between ice, snow, and water, which are ultimately driven by temperature forcing and the melt-elevation feedback. In our model, supraglacial lakes develop as a result of ice melting and accumulate in the depressions of the ice profile due to gravity, which is described by our novel algorithm.

https://doi.org/10.5194/egusphere-2025-6334
Preprint. Discussion started: 20 January 2026
© Author(s) 2026. CC BY 4.0 License.

The model shows that snow accumulation determines how the feedback is initiated. Low amounts of snow can only "shield" the bare ice and delay its melting, while abundant snow can completely prevent ice melt. In such cases, lakes can still contribute to mass loss from the Greenland Ice Sheet by removing water from the surface. This process implies that certain parameter ranges are necessary for melting to occur. Specifically, temperatures must be high enough to melt the snow entirely under the positive degree day scheme. Nevertheless, even with our simplified model, the melt lake feedback emerges clearly, highlighting the importance of including this process in large-scale Earth system models.

Our model presents some limitations (for example, supraglacial lakes cannot refreeze, whereas in reality this process often involves the formation of an ice lid at the lake surface). Supraglacial lakes also do not persist for multiple years in the model or alter the snow by producing slush as this state is not supported by the positive degree days scheme. However, we focused on simplicity to avoid interfering with the interesting result.

Future scenarios with higher greenhouse gas concentrations (e.g. SSP5-8.5) show earlier melting, which is further accelerated by supraglacial lake formation. In particular, CESM2 and NorESM2-MM temperature forcings produce different timings for the onset of the melt lake feedback in this scenario, indicating that structural differences between models can significantly affect ice sheet projections. However, under reasonable conditions, the models suggest that the melt-induced feedback loop enhanced by lake formation may become a dominant contributor to Greenland mass loss as early as the end of the century.

*Code availability.* Our Python code for a simple realization of the model run is available on Zenodo https://zenodo.org/records/17413871.

*Data availability.* We used no new datasets for this manuscript. The datasets for the projections of future scenarios can be found at (Norwegian Climate Centre, 2019; NCAR, 2020)

*Author contributions.* AC designed the study, implemented the simulations, and analyzed the results. UF and AH supervised the project, provided critical guidance on methodology, contributed to the interpretation of the results, and supported the work with data and dynamical modeling. All authors contributed to writing and revising the manuscript.

*Competing interests.* The authors declare that no competing interests are present.

*Acknowledgements.* This work was supported by the UiT Aurora Centre Program, UiT The Arctic University of Norway (2024), the Research Council of Norway (project number 314570). The authors of this manuscript wish to thank Ann Kristin Klose, Rajat Karnatak and Ricarda Winkelmann for the valuable suggestions that led to the improvement of this manuscript. UF acknowledges support from the Horizon 2020 Maria Skłodowska-Curie ITN Critical Earth (grant number 956170).

https://doi.org/10.5194/egusphere-2025-6334
Preprint. Discussion started: 20 January 2026
© Author(s) 2026. CC BY 4.0 License.

## References

Banwell, A. F., Arnold, N. S., Willis, I. C., Tedesco, M., and Ahlstrøm, A. P.: Modeling supraglacial water routing and lake filling on the Greenland Ice Sheet, Journal of Geophysical Research: Earth Surface, 117, https://doi.org/https://doi.org/10.1029/2012JF002393, 2012.

Boers, N.: Early-warning signals for Dansgaard–Oeschger events in a high-resolution climate record, Nature Communications, 9, 2556, https://doi.org/10.1038/s41467-018-04881-7, 2018.

Boers, N., Ghil, M., and Stocker, T. F.: Theoretical and paleoclimatic evidence for abrupt transitions in the Earth system, Environmental Research Letters, 17, 093 006, https://doi.org/10.1088/1748-9326/ac8944, 2022.

Box, J. E., Fettweis, X., Stroeve, J. C., Tedesco, M., Hall, D. K., and Steffen, K.: Greenland ice sheet albedo feedback: thermodynamics and atmospheric drivers, The Cryosphere, 6, 821–839, https://doi.org/10.5194/tc-6-821-2012, 2012.

Braithwaite, R. J.: Positive degree-day factors for ablation on the Greenland ice sheet studied by energy-balance modelling, Journal of Glaciology, 41, 153–160, https://doi.org/10.3189/S0022143000017846, 1995.

Buzzard, S. C., Feltham, D. L., and Flocco, D.: A Mathematical Model of Melt Lake Development on an Ice Shelf, Journal of Advances in Modeling Earth Systems, 10, 262–283, https://doi.org/https://doi.org/10.1002/2017MS001155, 2018.

Cessi, P.: A Simple Box Model of Stochastically Forced Thermohaline Flow, Journal of Physical Oceanography, 24, 1911 – 1920, https://doi.org/10.1175/1520-0485(1994)024<1911:ASBMOS>2.0.CO;2, 1994.

Charbit, S., Paillard, D., and Ramstein, G.: Amount of CO2 emissions irreversibly leading to the total melting of Greenland, Geophysical Research Letters, 35, https://doi.org/https://doi.org/10.1029/2008GL033472, 2008.

Christoffersen, P., Bougamont, M., Hubbard, A., Doyle, S. H., Grigsby, S., and Pettersson, R.: Cascading lake drainage on the Greenland Ice Sheet triggered by tensile shock and fracture, Nature Communications, 9, 1064, https://doi.org/10.1038/s41467-018-03420-8, 2018.

Chudley, T. R., Christoffersen, P., Doyle, S. H., Bougamont, M., Schoonman, C. M., Hubbard, B., and James, M. R.: Supraglacial lake drainage at a fast-flowing Greenlandic outlet glacier, Proceedings of the National Academy of Sciences, 116, 25 468–25 477, https://doi.org/10.1073/pnas.1913685116, 2019.

Cuffey, K. M. and Paterson, W. S. B.: The Physics of Glaciers, Academic Press, Amsterdam, 4th edn., ISBN 978-0123694614, 2010.

Diamond, R., Schroeder, D., Sime, L. C., Ridley, J., and Feltham, D.: The Significance of the Melt-Pond Scheme in a CMIP6 Global Climate Model, Journal of Climate, 37, 249 – 268, https://doi.org/10.1175/JCLI-D-22-0902.1, 2024.

dos Santos, T. D., Morlighem, M., and Seroussi, H.: Assessment of numerical schemes for transient, finite-element ice flow models using ISSM v4.18, Geoscientific Model Development, 14, 2545–2573, https://doi.org/10.5194/gmd-14-2545-2021, 2021.

Echelmeyer, K., Clarke, T. S., and Harrison, W.: Surficial glaciology of Jakobshavns Isbræ, West Greenland: Part I. Surface morphology, Journal of Glaciology, 37, 368–382, https://doi.org/10.3189/S0022143000005803, 1991.

Glen, J. W.: Experiments on the Deformation of Ice, Journal of Glaciology, 2, 111–114, https://doi.org/10.3189/S0022143000034067, 1952.

Greve, R. and Blatter, K.: Dynamics of Ice Sheets and Glaciers, Advances in Geophysical and Environmental Mechanics and Mathematics, Springer, 2009.

Hoffman, M. J., Perego, M., Andrews, L. C., Price, S. F., Neumann, T. A., Johnson, J. V., Catania, G., and Lüthi, M. P.: Widespread Moulin Formation During Supraglacial Lake Drainages in Greenland, Geophysical Research Letters, 45, 778–788, https://doi.org/https://doi.org/10.1002/2017GL075659, 2018.

https://doi.org/10.5194/egusphere-2025-6334
Preprint. Discussion started: 20 January 2026
© Author(s) 2026. CC BY 4.0 License.

Holland, M. M., Bailey, D. A., Briegleb, B. P., Light, B., and Hunke, E.: Improved Sea Ice Shortwave Radiation Physics in CCSM4: The Impact of Melt Ponds and Aerosols on Arctic Sea Ice, Journal of Climate, 25, 1413 – 1430, https://doi.org/10.1175/JCLI-D-11-00078.1, 2012.

Humbert, A., Helm, V., Zeising, O., Neckel, N., Braun, M. H., Khan, S. A., Rückamp, M., Steeb, H., Sohn, J., Bohnen, M., and Müller, R.: Insights into supraglacial lake drainage dynamics: triangular fracture formation, reactivation and long-lasting englacial features, The Cryosphere, 19, 3009–3032, https://doi.org/10.5194/tc-19-3009-2025, 2025.

Huybrechts, P., Letreguilly, A., and Reeh, N.: The Greenland ice sheet and greenhouse warming, Palaeogeography, Palaeoclimatology, Palaeoecology, 89, 399–412, https://doi.org/https://doi.org/10.1016/0031-0182(91)90174-P, 1991.

Khan, S. A., Seroussi, H., Morlighem, M., Colgan, W., Helm, V., Cheng, G., Berg, D., Barletta, V. R., Larsen, N. K., Kochtitzky, W., van den Broeke, M., Kjær, K. H., Aschwanden, A., Noël, B., Box, J. E., MacGregor, J. A., Fausto, R. S., Mankoff, K. D., Howat, I. M., Oniszk, K., Fahrner, D., Løkkegaard, A., Lippert, E. Y. H., Bråtner, A., and Hassan, J.: Smoothed monthly Greenland ice sheet elevation changes during 2003–2023, Earth System Science Data, 17, 3047–3071, https://doi.org/10.5194/essd-17-3047-2025, 2025.

Klose, A. K., Donges, J. F., Feudel, U., and Winkelmann, R.: Rate-induced tipping cascades arising from interactions between the Greenland Ice Sheet and the Atlantic Meridional Overturning Circulation, Earth System Dynamics, 15, 635–652, https://doi.org/10.5194/esd-15-635-2024, 2024.

Levermann, A. and Winkelmann, R.: A simple equation for the melt elevation feedback of ice sheets, The Cryosphere, 10, 1799–1807, https://doi.org/10.5194/tc-10-1799-2016, 2016.

Lüthje, M., Feltham, D. L., Taylor, P. D., and Worster, M. G.: Modeling the summertime evolution of sea-ice melt ponds, Journal of Geophysical Research: Oceans, 111, https://doi.org/https://doi.org/10.1029/2004JC002818, 2006a.

Lüthje, M., Pedersen, L., Reeh, N., and Greuell, W.: Modelling the evolution of supraglacial lakes on the West Greenland ice-sheet margin, Journal of Glaciology, 52, 608–618, https://doi.org/10.3189/172756506781828386, 2006b.

Machguth, H., Tedstone, A., Kuipers Munneke, P., Brils, M., Noël, B., Clerx, N., Jullien, N., Fettweis, X., and van den Broeke, M.: Runoff from Greenland's firn area – why do MODIS, RCMs and a firn model disagree?, EGUsphere, 2024, 1–33, https://doi.org/10.5194/egusphere-2024-2750, 2024.

Maier, N., Andersen, J. K., Mouginot, J., Gimbert, F., and Gagliardini, O.: Wintertime Supraglacial Lake Drainage Cascade Triggers Large-Scale Ice Flow Response in Greenland, Geophysical Research Letters, 50, e2022GL102 251, https://doi.org/https://doi.org/10.1029/2022GL102251, e2022GL102251 2022GL102251, 2023.

Marshall, S. J. and Sharp, M. J.: Temperature and Melt Modeling on the Prince of Wales Ice Field, Canadian High Arctic, Journal of Climate, 22, 1454 – 1468, https://doi.org/10.1175/2008JCLI2560.1, 2009.

Masson-Delmotte, V., Swingedouw, D., Landais, A., Seidenkrantz, M.-S., Gauthier, E., Bichet, V., Massa, C., Perren, B., Jomelli, V., Adalgeirsdottir, G., Hesselbjerg Christensen, J., Arneborg, J., Bhatt, U., Walker, D. A., Elberling, B., Gillet-Chaulet, F., Ritz, C., Gallée, H., van den Broeke, M., Fettweis, X., de Vernal, A., and Vinther, B.: Greenland climate change: from the past to the future, WIREs Climate Change, 3, 427–449, https://doi.org/https://doi.org/10.1002/wcc.186, 2012.

Mohanty, L. K. and Maiti, S.: Glacial lake formation probability mapping in the Himalayan glacier: A probabilistic modeling approach, Journal of Earth System Science, 131, 54, https://doi.org/10.1007/s12040-021-01772-2, 2022.

Morlighem, M., Williams, C. N., Rignot, E., An, L., Arndt, J. E., Bamber, J. L., Catania, G., Chauché, N., Dowdeswell, J. A., Dorschel, B., Fenty, I., Hogan, K., Howat, I., Hubbard, A., Jakobsson, M., Jordan, T. M., Kjeldsen, K. K., Millan, R., Mayer, L., Mouginot, J., Noël, B. P. Y., O'Cofaigh, C., Palmer, S., Rysgaard, S., Seroussi, H., Siegert, M. J., Slabon, P., Straneo, F., van den Broeke, M. R.,

https://doi.org/10.5194/egusphere-2025-6334
Preprint. Discussion started: 20 January 2026
© Author(s) 2026. CC BY 4.0 License.

Weinrebe, W., Wood, M., and Zinglersen, K. B.: BedMachine v3: Complete Bed Topography and Ocean Bathymetry Mapping of Greenland From Multibeam Echo Sounding Combined With Mass Conservation, Geophysical Research Letters, 44, 11,051–11,061, https://doi.org/https://doi.org/10.1002/2017GL074954, 2017.

NCAR: CESM2 model output prepared for CMIP6, ScenarioMIP. Experiments ssp126, ssp245, ssp370, ssp585. Ensemble member r10i1p1f1, variable ts (Surface Temperature), monthly data (2015–2100). Distributed via the Earth System Grid Federation (ESGF), https://doi.org/10.5065/D67H1H0V, 2020.

Norwegian Climate Centre: NorESM2-MM model output prepared for CMIP6 ScenarioMIP experiments. Experiments ssp126, ssp245, ssp370, ssp585. Ensemble member r1i1p1f1, variable: tas, monthly data on native grid (gn), downloaded via CDS API, https://doi.org/10.22033/ESGF/CMIP6.7085947c-8246-417c-8fee-bb6fe5ee600b, 2019.

O'Neill, B. C., Tebaldi, C., van Vuuren, D. P., Eyring, V., Friedlingstein, P., Hurtt, G., Knutti, R., Kriegler, E., Lamarque, J.-F., Lowe, J., Meehl, G. A., Moss, R., Riahi, K., and Sanderson, B. M.: The Scenario Model Intercomparison Project (ScenarioMIP) for CMIP6, Geoscientific Model Development, 9, 3461–3482, https://doi.org/10.5194/gmd-9-3461-2016, 2016.

Parizek, B. R. and Alley, R. B.: Implications of increased Greenland surface melt under global-warming scenarios: ice-sheet simulations, Quaternary Science Reviews, 23, 1013–1027, https://doi.org/https://doi.org/10.1016/j.quascirev.2003.12.024, 2004.

Pollard, D.: A simple parameterization for ice sheet ablation rate, Tellus, 32, 384–388, https://doi.org/https://doi.org/10.1111/j.2153-3490.1980.tb00965.x, 1980.

Rantanen, M., Karpechko, A. Y., Lipponen, A., Nordling, K., Hyvärinen, O., Ruosteenoja, K., Vihma, T., and Laaksonen, A.: The Arctic has warmed nearly four times faster than the globe since 1979, Communications Earth & Environment, 3, 168, https://doi.org/10.1038/s43247-022-00498-3, 2022.

Reeh, N.: Parameterization of melt rate and surface temperature on the Greenland Ice Sheet, Polarforschung, 59, 113–128, 1989.

Scagliarini, A., Calzavarini, E., Mansutti, D., and Toschi, F.: Modelling Sea Ice and Melt Ponds Evolution: Sensitivity to Microscale Heat Transfer Mechanisms, pp. 179–198, Springer International Publishing, Cham, ISBN 978-3-030-38669-6, https://doi.org/10.1007/978-3-030-38669-6_6, 2020.

Scott, F. and Feltham, D. L.: A model of the three-dimensional evolution of Arctic melt ponds on first-year and multiyear sea ice, Journal of Geophysical Research: Oceans, 115, https://doi.org/https://doi.org/10.1029/2010JC006156, 2010.

Smeets, P. C. J. P., Kuipers Munneke, P., van As, D., van den Broeke, M. R., Boot, W., Oerlemans, H., and van de Wal, R. S. W.: The K-transect in west Greenland: Automatic weather station data (1993–2016), Arctic, Antarctic, and Alpine Research, 50, https://doi.org/10.1080/15230430.2017.1420954, 2018.

Smith, D. M., Screen, J. A., Deser, C., Cohen, J., Fyfe, J. C., García-Serrano, J., Jung, T., Kattsov, V., Matei, D., Msadek, R., Peings, Y., Sigmond, M., Ukita, J., Yoon, J.-H., and Zhang, X.: The Polar Amplification Model Intercomparison Project (PAMIP) contribution to CMIP6: investigating the causes and consequences of polar amplification, Geoscientific Model Development, 12, 1139–1164, https://doi.org/10.5194/gmd-12-1139-2019, 2019.

Sneed, W. A. and Hamilton, G. S.: Evolution of melt pond volume on the surface of the Greenland Ice Sheet, Geophysical Research Letters, 34, https://doi.org/https://doi.org/10.1029/2006GL028697, 2007.

Stevens, L. A., Behn, M. D., McGuire, J. J., Das, S. B., Joughin, I., Herring, T., Shean, D. E., and King, M. A.: Greenland supraglacial lake drainages triggered by hydrologically induced basal slip, Nature, 522, 73–76, https://doi.org/10.1038/nature14480, 2015.

https://doi.org/10.5194/egusphere-2025-6334
Preprint. Discussion started: 20 January 2026
© Author(s) 2026. CC BY 4.0 License.

Tedesco, M., Lüthje, M., Steffen, K., Steiner, N., Fettweis, X., Willis, I., Bayou, N., and Banwell, A.: Measurement and modeling of ablation of the bottom of supraglacial lakes in western Greenland, Geophysical Research Letters, 39, https://doi.org/https://doi.org/10.1029/2011GL049882, 2012.

Trusel, L. D., Das, S. B., Osman, M. B., Evans, M. J., Smith, B. E., Fettweis, X., McConnell, J. R., Noël, B. P. Y., and van den Broeke, M. R.: Nonlinear rise in Greenland runoff in response to post-industrial Arctic warming, Nature, 564, 104–108, https://doi.org/10.1038/s41586-018-0752-4, 2018.

Tsai, V. C. and Ruan, X.: A simple physics-based improvement to the positive degree day model, Journal of Glaciology, 64, 661–668, https://doi.org/10.1017/jog.2018.55, 2018.

van den Berg, J., van de Wal, R., and Oerlemans, H.: A mass balance model for the Eurasian Ice Sheet for the last 120,000 years, Global and Planetary Change, 61, 194–208, https://doi.org/https://doi.org/10.1016/j.gloplacha.2007.08.015, 2008.

Zeitz, M., Haacker, J. M., Donges, J. F., Albrecht, T., and Winkelmann, R.: Dynamic regimes of the Greenland Ice Sheet emerging from interacting melt–elevation and glacial isostatic adjustment feedbacks, Earth System Dynamics, 13, 1077–1096, https://doi.org/10.5194/esd-13-1077-2022, 2022.

Zhang, Y., Liu, S., Xie, C., and Ding, Y.: Application of a degree-day model for the determination of contributions to glacier meltwater and runoff near Keqicar Baqi glacier, southwestern Tien Shan, Annals of Glaciology, 43, 280–284, https://doi.org/10.3189/172756406781812320, 2006.

Zwally, H. J., Abdalati, W., Herring, T., Larson, K., Saba, J., and Steffen, K.: Surface Melt-Induced Acceleration of Greenland Ice-Sheet Flow, Science, 297, 218–222, https://doi.org/10.1126/science.1072708, 2002.

https://doi.org/10.5194/egusphere-2025-6334
Preprint. Discussion started: 20 January 2026
© Author(s) 2026. CC BY 4.0 License.

**Table A1.** Other parameters in our program with variable names in the code, values, units, and short descriptions. We organize the table into five categories for better readability: Spatial and Domain Parameters, Solver and Integration Parameters, Time and Resolution Parameters, Initial Conditions, and Flags and Outputs.

| Variable (program) | Value | Unit | Explanation |
|---|---|---|---|
| `size` | 1000 | - | Number of spatial points |
| `d_ext` | 40000 | m | Domain spatial extent |
| `dx` | `d_ext`/size | m | Spatial resolution |
| `rtol` | 0.0001 | - | Solver relative tolerance |
| `atol` | $1 \times 10^{-8}$ | - | Solver absolute tolerance |
| `max_step` | 10000 | - | Maximum integrator step size |
| `tolerance_a` | $10^{-11}$ | - | Algorithm tolerance parameter $T_a$ |
| `tolerance_b` | $10^{-11}$ | - | Algorithm tolerance parameter $T_b$ |
| `y_ini_pr` | 10 | years | Initial profile evolution duration |
| `ini_pr_res` | 10000 | - | Profile resolution |
| `int_years` | 200 | years | Years of integration |
| `int_spinup` | 10 | years | Years of spin-up |
| `integ_res` | 100000 | - | Integration domain resolution |
| `num_chunks` | 50000 | - | Time chunks for water routine |
| `S_0` | 0.0 | m | Initial snow thickness |
| `W_0` | 0.0 | m | Initial water thickness |
| `I_0_M` | 690 | m | Initial mean ice thickness |
| `I_0_STD` | 50 | m | Initial std. dev. of ice thickness |
| `Wpresent` | True | - | Enables water formation and flow |
| `n_snap` | 10 | - | Snapshots per year for output |

## Appendix A: Other parameters used in our program

Table A1 shows the additional parameters used in our code, which define spatial resolution, solver tolerances, integration settings, and initial conditions for the simulations.

**A1**